

Hollow-Fiber Membrane-Based Rapid Pressure Swing Absorption

S. Bhaumik, S. Majumdar, and K. K. Sirkar

Dept. of Chemical Engineering, Chemistry and Environmental Science, New Jersey Institute of Technology,
Newark, NJ 07102

A novel gas purification technique called rapid pressure swing absorption (RAPSAB) was developed by integrating the best features of membrane contacting, gas-liquid absorption, and pressure swing adsorption (PSA). In this cyclic separation process, a well-packed microporous hydrophobic hollow-fiber module was used to achieve nondispersive gas absorption from a high-pressure feed gas into a stationary absorbent liquid on the module shell side during a certain part of the cycle followed by desorption of absorbed gases from the liquid in the rest of the cycle. The total cycle time varies between 20 s and upwards. Separation of mixtures of N_2 and CO_2 (around 10%) where CO_2 is the impurity to be removed was studied using absorbent liquids such as pure water and a 19.5% aqueous solution of diethanolamine (DEA). Three RAPSAB cycles studied differ in the absorption part. Virtually pure N_2 streams were obtained with DEA as absorbent demonstrating the capability of bulk separation to very high levels of purification. Numerical models developed predict the extent of purification for pure water and the DEA solution for one of the simpler cycles. Model simulations describe the observed behavior well.

Introduction

Large-scale separation of gas mixtures is achieved in a number of ways: absorption of gases in a reactive liquid, pressure swing adsorption (PSA) processes on a solid adsorbent, cryogenic processes, selective permeation through a membrane, and so on. Each such process has some real advantages and disadvantages. For example, membrane processes are compact, energy-efficient, modular, and economically attractive. They have low operating and capital costs. However, they are generally highly effective for bulk separation of gases and unsuitable for high levels of purification. PSA processes (Yang, 1987) are, however, highly efficient for removing small amount of impurities compared to other processes (Beaver and Bhat, 1988). The devices are generally bulky. The process becomes costly when the concentration of impurity to be removed increases given the lower selectivities of the existing adsorbents. These processes also require a large number of beds in practice.

Separation of gas mixtures using absorption in a reactive liquid is generally carried out in a packed tower or a tray

tower of which there are two, one for absorption and one for stripping. Due to poor contacting efficiencies, such a process involves large contactors which are costly and highly capital intensive (Spilman, 1989; Qi and Cussler, 1985); further, they suffer from flooding, loading, foaming, weeping, and so on.

Recently developed membrane-based gas-liquid contacting processes (Qi and Cussler, 1985) avoid such shortcomings (Sirkar, 1992). It is usually carried out in microporous hollow fiber-based systems to provide a very high interfacial area per unit volume. There are no problems of flooding, loading, foaming, and so on in such processes. Membrane-based gas-liquid contacting processes, however, require two vessels, one for absorption and the other for stripping. It has been observed that the shell-side liquid flow in such devices is subject to considerable bypassing (Karoor, 1992; Karoor and Sirkar, 1993; Yang and Cussler, 1986). This reduces separation considerably and necessitates newer module designs. Further, adsorption processes are generally recognized to be superior from the point of view of purification of a stream.

This article is concerned with a novel gas separation process concept. It incorporates the major strengths of a number of different gas separation techniques discussed above to cre-

Correspondence concerning this article should be addressed to K. K. Sirkar.

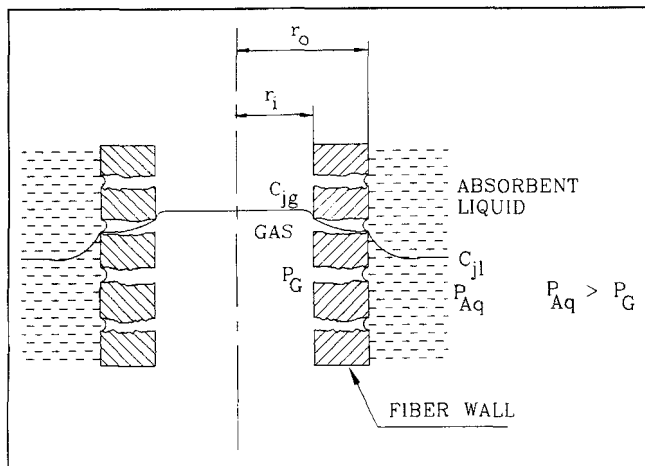


Figure 1. Concentration profile for absorbed species in gas and liquid phases.

ate a compact, energy-efficient, and modular process with high flux, separation factors, and purification capabilities. The process utilizes a microporous hydrophobic hollow fiber gas-liquid contactor in the manner of a PSA with the adsorbent liquid being stationary on the shell side and the gas flowing through the tube side. The liquid on the shell side replaces the traditional adsorbent particles in PSA. The liquid does not wet the hydrophobic fiber pores. The feed gas is made to flow through the fiber bore during one part of the cycle. The gas species comes in contact with the absorbent liquid on the fiber OD (Figure 1), where it is absorbed. During the rest of the cycle, no feed gas flows into the system; rather, the absorbed gas is removed from the absorbent liquid by pulling a vacuum. The desorbed gas flows out in a direction opposite to that of the feed gas flow. When such a cycle is of short duration, we can call the process rapid pressure swing absorption or RAPSAB in short.

Consider, for the sake of illustration, removal of an acid gas CO_2 from, say, N_2 by an absorbent liquid which is highly selective for CO_2 . As feed gas is introduced into the fiber bore at the feed end, CO_2 is absorbed and the gas leaving through the other fiber end is highly purified N_2 . After some time, the feed gas flow is stopped. Next, a vacuum is pulled to desorb the CO_2 present in the absorbent liquid through the feed end to prepare the absorbent liquid for the next cycle of absorption and desorption. Commercial PSA cycles for a similar problem will be somewhat more complex (Kikinides et al., 1993; Kumar and van Sloun, 1989). For example, there will be a high-pressure rinse step at the end of adsorption by a high-purity CO_2 stream flowing in the same direction as the feed gas. This step improves N_2 recovery, as well as production of high purity CO_2 during the next vacuum desorption step. There is an additional step in such PSA where high-purity high-pressure N_2 stream is introduced at the start of the cycle when pressurization occurs. Although such steps are important from the point of view of high recovery of N_2 and higher purity of the CO_2 stream, our objective here is focused on the core RAPSAB part of the cycle.

The proposed system has many advantageous features:

- An extremely high surface area/volume (up to 100 cm^{-1}) can be packed in the device using hollow fine fibers (ID, 100

μm ; OD, 150 μm). Bypassing or channeling of liquids on the shell side is eliminated.

- Extremely high purification capabilities of PSA or gas scrubbing processes are retained.

- The flooding-loading limitations of absorption towers are absent. The process can be applied to gas at any pressure (as in a membrane process) by employing proper pressure control on the liquid phase *vis-a-vis* the immobilized gas-liquid interfaces at the hollow-fiber pore mouths. For higher ΔP s, porous hollow fibers having a highly gas permeable non-porous coating may be employed (Papadopoulos and Sirkar, 1994).

- Extraordinarily large inventory of liquid absorbents may be tapped for almost any separation desired. The absorption capacity and selectivity of liquids, especially reactive ones, are considerably larger than most adsorbents.

- One vessel replaces two vessels, an absorber and a stripper used in conventional absorption processes. Absorbent pumping is absent.

- By using very short time cycles, rates of absorption and desorption achieved are quite high since the rate is $\propto t^{-0.5}$.

Development of RAPSAB cycles requires special considerations. The hollow fiber bore provides a low-pressure drop channel without the form friction of conventional packed beds in PSA. Thus, development of pressure in the fiber bore requires somewhat different cycles; otherwise the high gas flow rate may overwhelm the absorption capacity of absorbent liquids and may not yield the desired purification level. We will, therefore, focus first on the nature of the RAPSAB cycles to be studied. The system studied here is the separation of a binary mixture of N_2 and CO_2 with CO_2 level being around 10%. The absorbent liquid employed is water and an aqueous solution (19.5%) of diethanolamine (DEA). We have also developed numerical models to predict the performance of the rapid gas absorption part of one of the simpler cycles. The models are valid for both physical absorption of CO_2 in water, as well as reactive absorption of CO_2 in aqueous DEA solutions. RAPSAB studies on removal of CO from N_2 and organic solvent vapor from air will be reported later.

Illustration of RAPSAB Cycles

To develop a perspective, we first illustrate the basic varieties of RAPSAB cycles of immediate interest. We consider three cycles identified as *mode 1*, *mode 2*, and *mode 3* since they are just different ways of carrying out the RAPSAB process. To describe these modes, we need the schematic of a hollow fiber module (HFM) as a black box with a few solenoid valves and a plot of how the pressure is varying in the fiber bore of the module through which the gas streams flow in one or the other direction.

Mode 1

High-pressure feed gas was allowed to enter for a certain time (such as 7 s) into the fiber bore through a two-way solenoid valve (2-WSV) 1 (Figure 2) keeping the other two 2-WSVs 2 and 3 closed. This corresponds to pressurization with feed step 1 shown in Figure 3. Then valve 1 was also closed, that is, the whole module was isolated for a brief period of time (such as 7 s) to introduce an artificial delay time during which absorption proceeds. This corresponds to "large

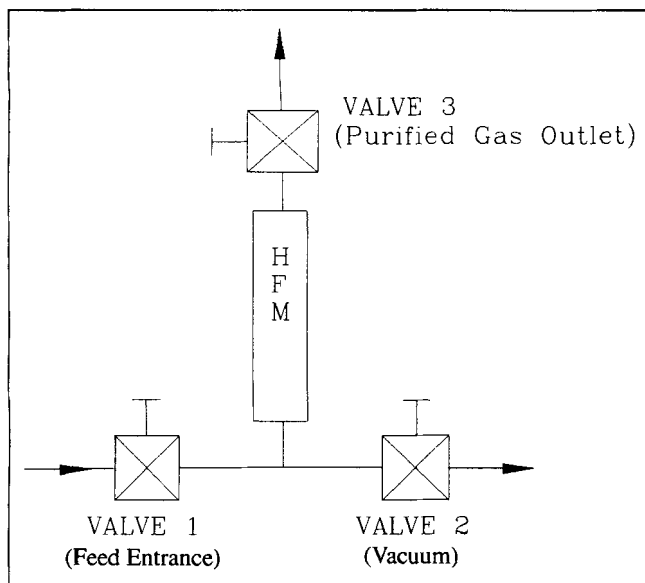


Figure 2. Solenoid valve locations in RAPSAB apparatus: modes 1 and 2.

delay," step 2 of Figure 3. Due to absorption, the gas pressure will decrease a little in step 2. Subsequently, valve 3 was opened momentarily (such as 4 s) to take out the purified gas. This corresponds to product withdrawal step 3 (Figure 3). Finally, valve 3 was allowed to close and simultaneously valve 2 was opened for vacuum desorption for, say, 20 s (step 4, Figure 3). This completed one whole cycle of operation. During vacuum desorption the gases flow out of the module through the feed end.

Mode 2

High-pressure feed gas was allowed to enter the fiber bores for a certain time (1 s) through valve 1 (Figure 2) until the

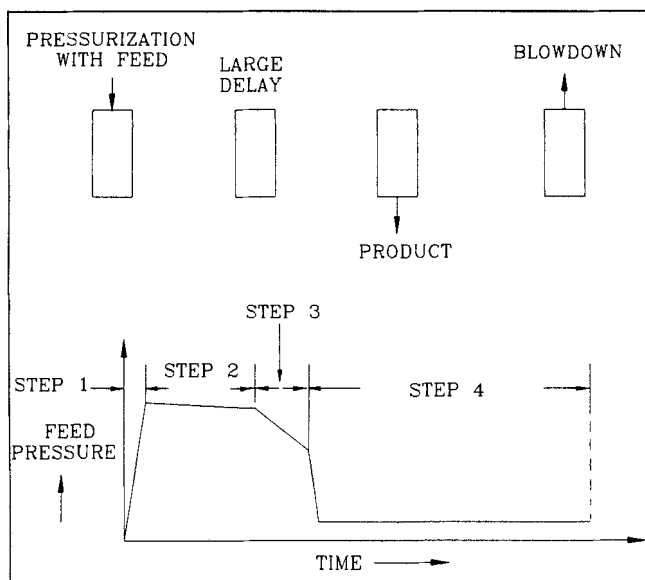


Figure 3. Pressure vs. time profile in hollow fiber bore: mode 1.

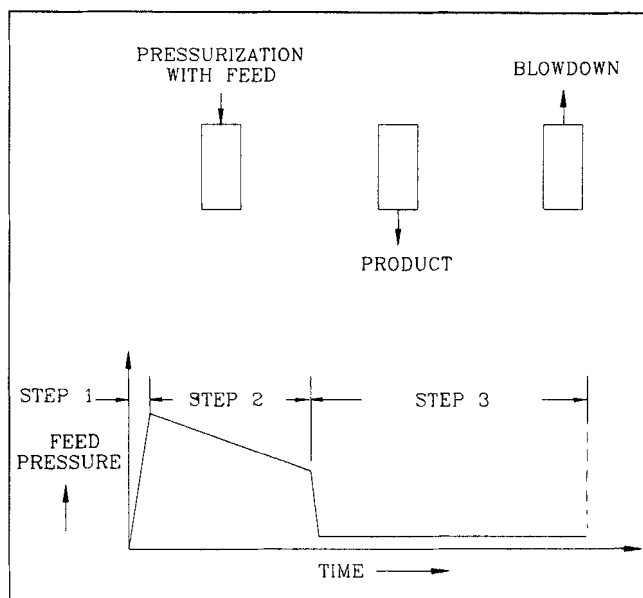


Figure 4. Pressure vs. time profile in hollow fiber bore: mode 2.

required pressure had been reached with both valves 2 and 3 being closed. This corresponds to step 1 pressurization with the feed in Figure 4. After that, valve 1 was closed and simultaneously valve 3 was opened for a short time (9 s) just to take out the purified front of the mixture of gases. This corresponds to step 2 of Figure 4 where the gas pressure in fiber bore decreases slowly with time. [Note the small delay in rapid pressure swing adsorption (Keller and Jones, 1980).] Then valve 3 was closed and simultaneously valve 2 was opened for vacuum desorption for, say, 20 s. This completed one whole cycle of operation. Step 2 of mode 1 does not exist in mode 2.

Mode 3

This mode of operation requires a different type of solenoid valve configuration shown in Figure 5. High-pressure feed gas mixture was allowed to enter the hollow fiber bore through the inlet end of a three-way solenoid valve (3-WSV) for a certain time (say, 15 s) while the purified product gas mixture was taken out through the 2-WSV at the exit end of the permeator. This corresponds to a combination of steps 1 and 2 in Figure 6. Then the 2-WSV at the product end and the inlet end of the 3-WSV were closed; simultaneously, the other end of the 3-WSV was opened for the vacuum desorption for a certain length of time (20 s). This corresponds to step 3 in Figure 6 at the end of which one complete cycle of operation is completed. Mode 3 is simpler in operation than modes 1 and 2 and is suitable for high capacity absorbent liquids. Modes 1 and 2 are much more suitable for low capacity absorbent liquids.

Experimental

Hollow-fiber modules

Rapid pressure swing absorption-separation of gas mixtures was carried out in a hollow fiber module shown in Figure 7. The module resembles a shell-and-tube heat exchanger

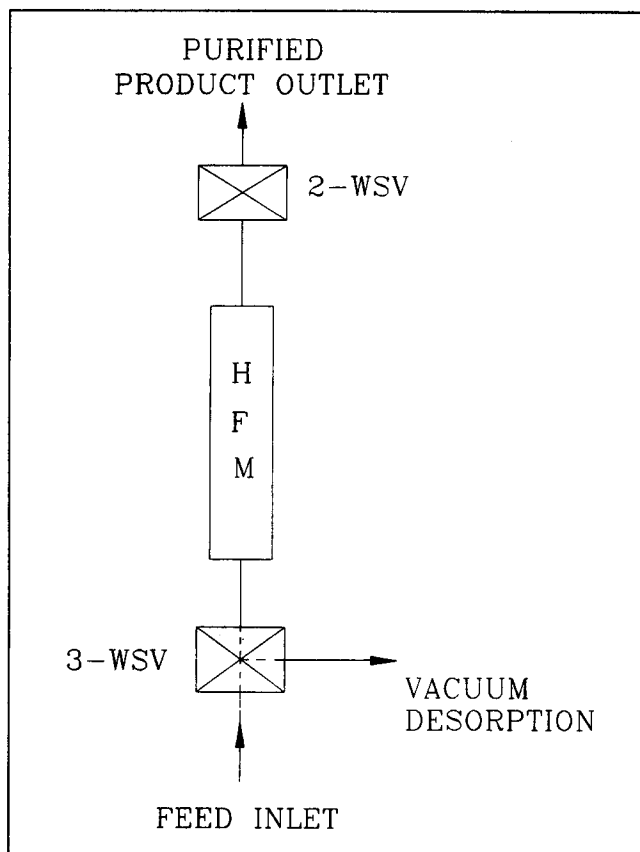


Figure 5. Solenoid valve locations in RAPSAB apparatus: mode 3.

without any baffles and contains a large number of micro-porous hydrophobic polypropylene hollow fibers (Celgard X-10, Hoechst Celanese Corp., Charlotte, NC). These fibers have $0.03\text{-}\mu\text{m}$ pore size. The fiber dimensions and the characteristics of two modules (4 and 5) fabricated and used are

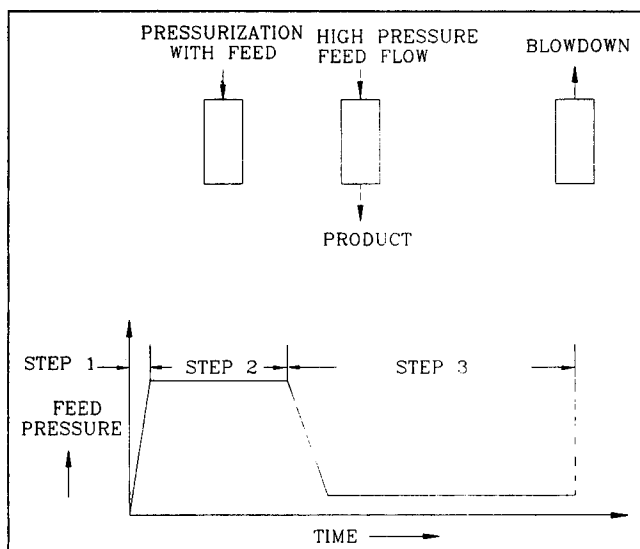


Figure 6. Pressure vs. time profile in hollow fiber bore: mode 3.

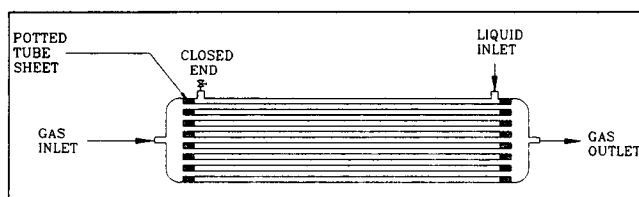


Figure 7. Hollow fiber module.

described in Table 1. In general, fabrication of a HFM involved preparation of a fiber bundle, inserting it in a shell and potting the ends of fiber set with a resin mixture to form a tube sheet. Prior to potting the fibers in the shell, tests were done to check fiber leakage; after potting the fibers in the shell, leakage test was again carried out to make sure that the module was functional. Further details are provided by Bhaumik et al. (1994).

Experimental setup for mode 3

RAPSAB study for the simpler operational mode (mode 3) was carried out in a setup shown in Figure 8. The apparatus had four segments: (i) feed gas line; (ii) purified gas line; (iii) stationary absorbent liquid line; (iv) vacuum line; all segments were tied to a hollow fiber module. During the brief pressurization step at the start of a cycle, the feed gas mixture of a desired concentration was sent through a needle valve (R.S. Crum, Mountainside, NJ) and a 3-WSV (Components and Control, Carlstadt, NJ) to the tube side of the module. The pressure of the feed gas stream was indicated by a gauge (Matheson, E. Rutherford, NJ) before it was introduced into the module.

The purified feed stream exited through the other end of the module during the high-pressure feed flow part of the cycle and passed through a normally open 2-WSV (Components and Control, Carlstadt, NJ), and a check valve to the surge drum. The 3-WSV at the inlet and the two-way valve at the exit of the module were controlled by a single timer. The purified gas was then taken to the gas chromatograph (GC) (Model 3700, Varian, Palo Alto, CA) having a thermal conductivity detector to determine its composition. Porapak N 80/100 mesh columns were used. The flow rate of the purified gas stream after the surge drum was measured by a bubble flowmeter.

The absorbent liquid storage tank (LST) was pressurized by a N_2 gas cylinder. The liquid was introduced to the module shell side through a check valve and a regulating valve. The exit regulating valve on the shell side was kept closed

Table 1. Characteristics of Hollow-Fiber Modules

Module No.	4	5
Effective Length, cm	160	160
No. of Fibers	1,198	840
ID, μm	100	100
OD, μm	150	150
Surface Area, cm^2	9,033	6,333
Area/Vol., cm^{-1}	29	136
Void Fraction	0.89	0.49*

*A Teflon pipe (ID: 0.61cm; OD: 1.03 cm) was used to contain the fibers in a defined volume.

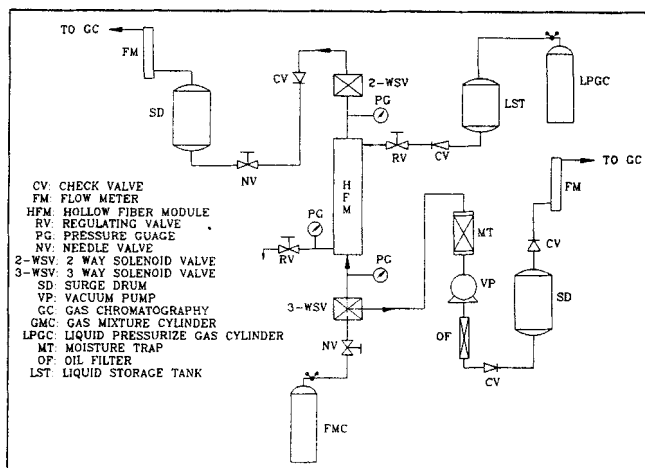


Figure 8. Setup for RAPSAB experiments in mode 3.

during operation as the absorbent was stationary. This valve was used to drain the liquid during shutdown. The pressure of the absorbent liquid was maintained at a level of 35-70 kPa higher than the feed gas stream pressure so that the liquid did not wet the fiber pores. This was the case as the modules made of microporous hydrophobic polypropylene hollow fibers were used with water as an absorbent for the gas mixture separation.

During the next part of the cycle (which starts with blow-down), the supply of the feed gas to the module was terminated by the 3-WSV. The purified gas line was also detached from the module by shutting the 2-WSV in the exit line for the purified gas stream. The desorbed gas was taken out by a vacuum pump (VP) through the feed end of the module and through the alternate channel of the 3-WSV. The moisture in this desorbed gas stream was removed by a Drierite column before the gas was sucked into the vacuum pump. The gas stream was then sent through an oil filter, a check valve, another surge drum and another valve respectively. The gas stream flow rate would be measured by an electronic flowmeter before its composition was determined by the GC. To minimize the dead volume in the connecting lines, a thick walled polypropylene tubing (Imperial Eastman, Chicago) of 0.32 cm OD was utilized for connecting different equipment with minimum length.

Experimental setup for modes 1 and 2

To increase the rate of gas absorption in the stagnant absorbent liquid, it was necessary to raise the pressure in a relatively short period of time. To build up higher feed gas pressure in the fiber lumen, a few changes were incorporated in the experimental setup of Figure 8 where only one electronic timer was used to control two solenoid valves: the two-way solenoid valve at the exit end of the permeator and the three-way solenoid valve at the permeator inlet end. Therefore, both valves would open and close simultaneously; this prevented a large pressure build up in the fiber lumen since there was very little flow pressure drop in the fiber lumen. If the solenoid valve at the exit end could be kept closed for some time when the feed gas was flowing into the fiber bore through the other end, it would then be possible to build up a certain pressure in the fiber lumen within a short time. Further, it is

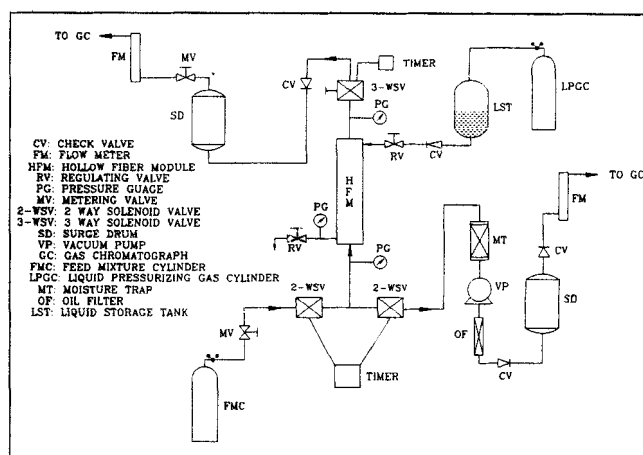


Figure 9. Setup for RAPSAB experiments in modes 1 and 2.

not an imperative that the feed has to be supplied for the given absorption time but it can be supplied only for a few seconds and then stopped; then the purified gas stream can be taken out through the exit end of the permeator.

Therefore, instead of a 3-WSV at the feed inlet side of the permeator, two normally closed 2-WSVs (Components and Control, Carlstadt, NJ) were installed; one for the feed inlet and the other for the vacuum desorption line. At the exit end of the permeator one 3-WSV with one end closed was installed instead of the 2-WSV to serve the purpose. One timer controlled two 2-WSV solenoid valves at the permeator inlet end and a new timer controlled the 3-WSV at the permeator exit end. The modified experimental setup is shown in Figure 9.

Experimental procedure

To start an experiment, the shell-side absorbent liquid (water or an aqueous solution of DEA) was first pressurized to a pressure slightly higher than the pressure of the feed gas entering the fiber lumen. The absorbent liquid was stationary on the shell side. The experiment was then started in any one of the operational modes described earlier (modes 1, 2 or 3).

The system was operated under a given cycle repeatedly for hundreds of such cycles over a period of three to eight hours. The product flow rate and composition were stabilized within one to three hours of operation and remained steady throughout the rest of the experimental run. The initial one to three hour period is required to expel air or existing gas mixture from the downstream connecting lines and the surge drum reservoir. The composition of the purified product stream was determined periodically by injecting gas samples from the surge drum into the GC. The flow rate of the purified gas was controlled by the metering valve after the surge drum. A steady state was considered achieved when no change in gas composition was noticed in at least five consecutive gas samples.

Models for RAPSAB

A simplified model has been developed for steps 1 and 2 of the RAPSAB operational mode 3 (Figure 6) carried out in a

hollow-fiber module shown in Figure 7. The gas or gas mixture is fed inside the fibers and the shell side is filled with an absorbent liquid which does not wet the fibers. The liquid is stationary and its pressure is higher than the gas pressure so that the gas-liquid phase interface is immobilized at each pore mouth on the OD of the microporous membrane (Figure 1). It is assumed that the hollow fibers are arranged in a regular pitch and the analysis based on a single fiber can be extended to the whole device. To this end, we consider the equivalent annulus or free surface model (Happel, 1959) to be valid. This model assumes a cylindrical fluid envelope surrounding each hollow fiber, that is, there exists two concentric cylinders: the inner cylinder consists of one hollow fiber and the outer cylinder consists of the absorbent liquid with a free surface (Figure 10) across which there is no mass transfer. This approximation of Happel's free surface model has been applied successfully to analyzing hollow fiber reverse osmosis systems (Gill and Bansal, 1973).

Model for water as absorbent

The following assumptions are introduced for absorption of gases into water in the RAPSAB system (steps 1 and 2 in mode 3).

- (1) Ideal gas law is valid.
- (2) The absorption process is isothermal.
- (3) Diffusion and solubility coefficients are constants and independent of concentration.
- (4) No reaction takes place between the liquid and any gas component.
- (5) The components of the gas phase are in equilibrium with the absorbed components at the gas-liquid interface and Henry's law is valid.
- (6) The flow pattern within the fiber bore can be described by the model of plug flow with axial diffusion.
- (7) The mass-transfer mechanism from the bulk gas phase to the outside surface of the fiber where the gas-liquid interface is located may be described by a first-order model based upon a constant mass-transfer coefficient and a concentration difference between the two locations.
- (8) The pressure drop in the fiber lumen is governed by the Hagen-Poiseuille equation for the compressible fluid without any effect of radial absorption.
- (9) The deformation of the fibers due to the higher external pressure of the liquid is negligible so that the fiber size and the void fraction remain unaltered.
- (10) End effects are negligible.
- (11) Volume of gas in the pores is negligible compared to that in the fiber lumen.

In determining the equivalent radius of free surface, we consider that the relative volume of absorbent liquid surrounding a single fiber is the same as the relative volume of the total liquid surrounding all hollow fibers in the module (Happel, 1959). If ϵ , the void fraction of the fiber bundle, is defined as

$$\epsilon = 1 - \frac{\text{shell-side cross-sectional area occupied by the hollow fibers } (= N\pi r_o^2)}{\text{total cross-sectional area of the shell side } (= \pi r_s^2)}$$

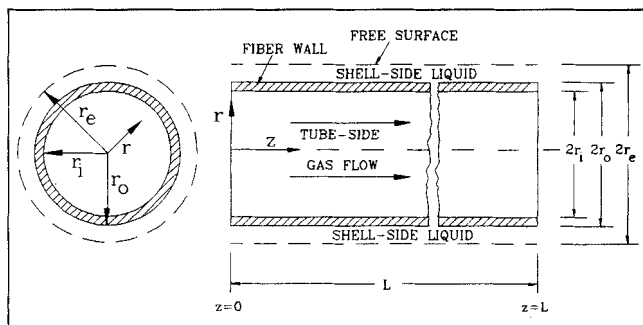


Figure 10. Representation of Happel's free surface model.

then one can easily obtain:

$$r_e = \left(\frac{1}{1 - \epsilon} \right)^{1/2} r_o \quad (1)$$

where r_e is the equivalent radius (Figure 10).

The differential mass balance equation for any species j in a single hollow fiber may be written as (Bhaumik et al., 1994):

$$\frac{\partial C_{jg}}{\partial t} + \frac{\partial [v_g C_{jg}]}{\partial z} + \frac{4K_{jg}d_o}{d_i^2} (C_{jg} - C_{jl}^i) = D_{jg} \frac{\partial^2 C_{jg}}{\partial z^2} \quad (2)$$

where

$$v_g = -\frac{RTd_i^2}{32\mu_g} \sum_{j=1}^n \frac{\partial C_{jg}}{\partial z}; \quad C_{jl}^i = \frac{C_{jl}|_{r=r_o}}{H_j RT} \quad (3)$$

Note that, in writing the balance equation, the ID of the hollow fiber is considered for the convection, diffusion and accumulation terms as the gas flow takes place inside the hollow fiber. However, the mass transfer between the gas and the absorbing liquid actually takes place on the fiber OD, hence the mass-transfer area for the absorption term is based on the OD of the hollow fiber. The boundary conditions and initial condition for any species j (N_2 , CO_2) in the gas phase are as follows:

Initial Condition:

$$\text{at } t = 0, C_{jg} = 0 (0 \leq z \leq L) \quad (4)$$

Boundary Conditions:

$$v_g C_{jg}|_u = v_g C_{jg}|_{z=0} - D_{jg} \frac{\partial C_{jg}}{\partial z} \Big|_{z=0} \quad (5a)$$

$$D_{jg} \frac{\partial C_{jg}}{\partial z} \Big|_{z=L} = 0 \quad (5b)$$

The corresponding differential equation for the liquid phase balance for species j is:

$$\frac{\partial C_{jl}}{\partial t} = D_{jl} \left(\frac{\partial^2 C_{jl}}{\partial r^2} + \frac{1}{r} \frac{\partial C_{jl}}{\partial r} \right) \quad (6)$$

Due to cylindrical symmetry, we have ignored any diffusion in the θ direction. The initial and boundary conditions are:

Initial Condition:

$$\text{at } t = 0, C_{jl} = 0 \quad (0 \leq z \leq L \text{ and } r_o < r < r_e) \quad (7)$$

Boundary Conditions:

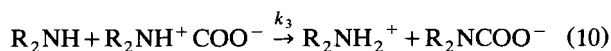
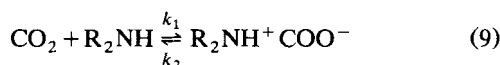
$$-D_{jl} \frac{\partial C_{jl}}{\partial r} \Big|_{r=r_o} = K_{jg} \left(C_{jg} - \frac{C_{jl}|_{r=r_o}}{H_j RT} \right) \quad (8a)$$

$$\frac{\partial C_{jl}}{\partial r} \Big|_{r=r_e} = 0 \quad (8b)$$

There are a variety of methods such as finite difference, orthogonal collocation, and method of lines available for the numerical solution of PDEs in time and spatial dimensions. We have adopted here the method of lines technique in which only the spatial gradients are discretized by finite difference equations thus reducing the system of PDEs to a coupled system of ODEs in the time domain (Brian et al., 1987). Following Brian et al. (1987), the effective absorption column length in the axial direction and the annular section between the fiber outside radius [$r = r_o \Rightarrow \eta = (r/r_e) = a$] and the free surface radius ($r = r_e \Rightarrow \eta = 1$) in the radial direction have been discretized into NB and NR points, respectively. The normalized distance between any two adjacent axial point is ΔX where $X = z/L$ (L being the module length) and that between two radial points is $\Delta \eta$. The procedure has transformed the nondimensional forms of Eqs. 2 and 6 for a single species to [NB + NB X NR] ordinary differential equations in normalized time parameter (Bhaumik et al., 1994).

Model development for a reactive system

Aqueous solution of diethanolamine (DEA) reacts reversibly with CO_2 . Sada et al. (1985) proposed the following reaction scheme for CO_2 absorption in an aqueous DEA solution:



The mechanism proposed has two steps: formation of zwitterion followed by the removal of a proton by amine. If steady-state approximation is applied to the unstable intermediates, then a homogeneous reaction rate (Sada et al., 1985) can be expressed as

$$r_{\text{CO}_2} = \frac{[\text{R}_2\text{NH}][\text{CO}_2]}{\frac{1}{k_1} + \frac{k_2}{k_1 k_3 [\text{R}_2\text{NH}]}} \quad (11)$$

If the first term in the denominator is much smaller than the second term, the reaction becomes second order with respect to amine and the rate constant becomes $k_1 k_3 / k_2$. On the other hand, if the first term is much larger than the second, the reaction will be first-order with respect to amine and the overall order will be second where the rate constant would be k_1 .

For this initial study, the reaction mechanism and the reaction rate expression proposed by Sada et al. (1985) are being considered and a simplified model for gas absorption in mode 3 has been developed using Happel's (1959) free surface model (guided by the modeling and results of Karoor, 1992). One fiber surrounded by reactive absorbents is considered in a unit cell of radius r_e . Gas flows through the fiber lumen. Gas pressure drop in the fiber lumen was also included in the model. The governing balance equations and boundary conditions for any species j (N_2 , CO_2) in the gas phase continue to be Eqs. 2, 3, 4, 5a and 5b.

In the liquid phase, now, there are at least three components to be considered: N_2 , CO_2 , and the amine. For N_2 , the mass balance and initial and boundary conditions are:

$$\frac{\partial C_{\text{N}_2 l}}{\partial t} = D_{\text{N}_2 l} \left(\frac{\partial^2 C_{\text{N}_2 l}}{\partial r^2} + \frac{1}{r} \frac{\partial C_{\text{N}_2 l}}{\partial r} \right) \quad (12)$$

Initial Condition:

$$\text{at } t = 0, C_{\text{N}_2 l} = 0 \quad (0 \leq z \leq L \text{ and } r_o < r < r_e) \quad (13)$$

Boundary Conditions:

$$-D_{\text{N}_2 l} \frac{\partial C_{\text{N}_2 l}}{\partial r} \Big|_{r=r_o} = K_{\text{N}_2 g} \left(C_{\text{N}_2 g} - \frac{C_{\text{N}_2 l}|_{r=r_o}}{H_{\text{N}_2} RT} \right) \quad (14)$$

$$\frac{\partial C_{\text{N}_2 l}}{\partial r} \Big|_{r=r_e} = 0 \quad (15)$$

The mass balance equation and the initial and boundary conditions for CO_2 (represented by A) in the liquid phase are:

$$\frac{\partial C_{Al}}{\partial t} = D_{Al} \left(\frac{\partial^2 C_{Al}}{\partial r^2} + \frac{1}{r} \frac{\partial C_{Al}}{\partial r} \right) - \frac{C_{Al} C_{Bl}}{\frac{1}{k_1} + \frac{k_2}{k_1 k_3 C_{Bl}}} \quad (16)$$

where diethanolamine has been represented as B.

Initial Condition:

$$C_{Al}(z, r, t = 0) = 0 \quad (17)$$

Boundary Conditions:

$$-D_{Al} \frac{\partial C_{Al}}{\partial r} \Big|_{r=r_o} = K_{Ag} \left(C_{Ag} - \frac{C_{Al}|_{r=r_o}}{H_A RT} \right) \quad (18)$$

$$\frac{\partial C_{Al}}{\partial r} \Big|_{r=r_e} = 0 \quad (19)$$

The mass balance equation with the initial and boundary conditions for DEA are

$$\frac{\partial C_{Bl}}{\partial t} = D_{Bl} \left(\frac{\partial^2 C_{Bl}}{\partial r^2} + \frac{1}{r} \frac{\partial C_{Bl}}{\partial r} \right) - \frac{2 C_{Al} C_{Bl}}{\frac{1}{k_1} + \frac{k_2}{k_1 k_3 C_{Bl}}} \quad (20)$$

Initial Condition:

$$C_{Bl}(z, r, t = 0) = C_{Bl0} \quad (21)$$

Boundary Conditions:

$$\frac{\partial C_{Bl}}{\partial r} \Big|_{r=r_o} = 0 \quad (22)$$

$$\frac{\partial C_{Bl}}{\partial r} \Big|_{r=r_e} = 0 \quad (23)$$

Partial differential Eqs. 2, 12, 16, and 20 are to be solved simultaneously along with the corresponding initial and boundary conditions identified above. They were solved in dimensionless form using the method of lines technique to convert the partial differential equations (PDEs) into ordinary differential equations (ODEs) in time and spatial dimensions. The computer codes were written in Fortran 77 using the IMSL subroutine, DIVPAG; the program was run in the mainframe computer, VAX/VMS environment.

Results and Discussion

A large number of preliminary experiments were carried out with water as the stationary absorbent for absorption of

CO₂ from a N₂-CO₂ gas mixture. This allowed the development of the cycles and evaluation of the comparative performance of the cycles. Afterwards, fewer experiments were carried out using 19.5% solution of DEA in water as the absorbent. The steady-state purification results will be presented and discussed first for water and then for the reactive DEA solution. Two items, namely, the extent of purification of the feed gas and the production rate of this high-pressure feed gas are of interest. Although the production rate and quality of the CO₂-rich stream obtained via vacuum desorption are also of interest, these aspects are not being covered here due to the nature of the RAPSAB cycles studied.

Water absorbent in modes 2 and 3

Experiments have been carried out in modes 2 and 3 with water as the absorbent by varying the time for the absorption part of the cycle. The desorption time was maintained always at 15 s since earlier studies indicated this to be the shortest time needed for effective desorption. The feed gas mixture contained either 10.2% or 9.9% CO₂, the balance being N₂. Modules 4 and 5 were used for mode 3 type of operation; only module 5 was used for mode 2 type of operation. The time duration for absorption and desorption part of the simple cycle in mode 3, the feed flow rate, and the purified product flow rate for all experiments are identified in Table 2 along with the purified gas composition in each case. The feed gas flow rate was kept constant for any given module as the absorption time was changed. One observes that as the absorption time increases the purified product gas flow rate increases; simultaneously, the CO₂ content of the purified outlet product gas increases signifying lower levels of purification. For module 4, an absorption time of 10 s yielded the best product quality, such as 2.5% CO₂. Whereas for module 5, which has a much larger surface area per unit volume, the same length of absorption time achieved a much lower CO₂ composition (1.48%).

The experimental data obtained with module 5 in mode 3 operation have been compared with the numerical model simulation results. They are identified in Figure 11. Normalized high-pressure exit compositions have been plotted against the normalized absorption time (D_{1l}/r_e^2). The experimental values of the purified gas flow rate for different nor-

Table 2. Experimental Results for Water Absorbent Using Modules 4 and 5 in Mode 3

Exp. No.	Module No.	Abs. Time (s)	Des. Time (s)	Feed Flow Rate (cm ³ /min)	Feed Pres. (kPa)	Product Outlet Comp.*	Product Flow Rate (cm ³ /min)
7-1	4	10	15	150	135 ~ 170	CO ₂ : 2.50%	~ 5
7-2	4	13	15	150	170 ~ 205	CO ₂ : 2.68%	~ 8
7-3	4	16	15	150	~ 205	CO ₂ : 2.95%	~ 18
7-4	4	20	15	150	205 ~ 240	CO ₂ : 3.12%	~ 25
7-5	5	10	15	120	~ 135	CO ₂ : 1.48%	~ 5
7-6	5	12	15	120	~ 170	CO ₂ : 1.82%	~ 10
7-7	5	15	15	120	~ 205	CO ₂ : 2.39%	~ 15
7-8	5	18	15	120	~ 240	CO ₂ : 2.85%	~ 22
7-9	5	19.5	15	120	~ 275	CO ₂ : 3.42%	~ 32
7-10	5	21	15	120	~ 310	CO ₂ : 4.55%	~ 40
7-11	5	22.5	15	120	~ 310	CO ₂ : 5.64%	~ 50
7-12	5	25	15	120	~ 310	CO ₂ : 6.90%	~ 60

Feed Composition: 10.2% CO₂-Balance N₂
 * Balance N₂

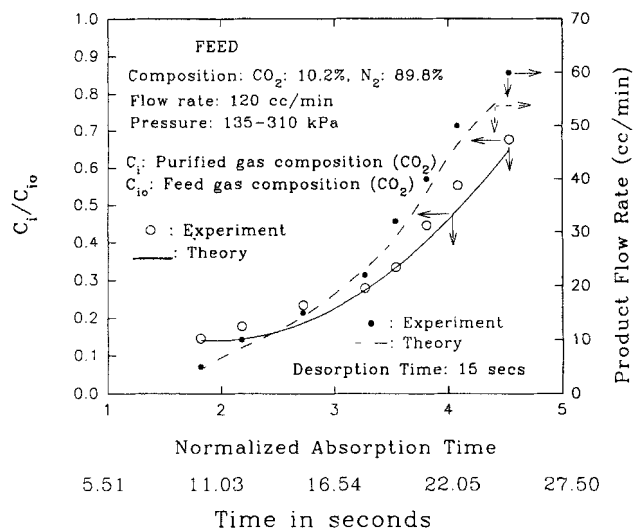


Figure 11. RAPSAB performance for the removal of CO₂ with water as an absorbent in mode 3: comparison with theoretical results.

malized absorption times are also compared with the simulation results in the same plot. The model predicts the experimental data reasonably well.

It is necessary to explain here why the exit CO₂ concentra-

tion increases as the absorption time increases. As feed stream flows through the fiber bore in the module, one component (CO₂) of the gas stream is absorbed much more in the absorbent water. The CO₂ concentration in the gas phase, therefore, decreases as the gas stream moves through the module and approaches zero at the exit of the module. So, at low values of absorption time, the purified gas stream has very little CO₂ as an impurity. However, the liquid in the module has a finite capacity for absorption. As the absorption time increases in different sets of experiments, the product CO₂ concentration increases. This behavior is similar to that of a PSA system. Note that each data point represents steady-state results over hundreds of cycles having a given absorption and desorption period.

The low absorption time in the above set of experiments are, however, characterized by a low level of gas pressure in the system (135 kPa), a severe deficiency. This suggested the need for a delay time during which the two way solenoid valve at the outlet would remain closed allowing the gas pressure to rise to high levels (modes 1 and 2).

Module 5 was, therefore, used for different experimental runs in mode 2 operation. The duration of the open and close settings of the solenoid valves and the corresponding values of the feed gas pressure have been identified in Table 3. The purification results for each such run identified in Table 3 are provided in Table 4. In the first set of experiments, the feed inlet metering valve was set at 800 cm³/min and the feed

Table 3. Duration of Different Settings of Solenoid Valves for Mode 2 Operation with Water in Module 5

Exp. No.	Module No.	Mode of Oper.	Pres. in Fiber Lumen (kPa)	Valve No. 1, s		Valve No. 3, s		Valve No. 2, s		Total Cycle Time, s
				Open	Close	Close	Open	Close	Open	
8-1	5	2	310 ~ 345	3	17	3	2	5	15	20
8-2	5	2	310 ~ 345	3	18	3	3	6	15	21
8-3	5	2	310 ~ 345	3	19	3	4	7	15	22
8-4	5	2	310 ~ 345	3	20	3	5	8	15	23
8-5	5	2	310 ~ 345	3	21.5	3	6.5	9.5	15	24.5
8-6	5	2	310 ~ 345	3	23	3	8	11	15	26
8-7	5	2	310 ~ 345	3	24	3	9	12	15	27
8-8	5	2	240 ~ 275	2	20.8	2	5.8	7.8	15	22.8
8-9	5	2	240 ~ 275	2	21.8	2	6.8	8.8	15	23.8
8-10	5	2	240 ~ 275	2	22.8	2	7.8	9.8	15	24.8
8-11	5	2	240 ~ 275	2	23.8	2	8.8	10.8	15	25.8
8-12	5	2	240 ~ 275	2	25	2	10	12	15	27

Table 4. Experimental Results for RAPSAB Using Water as Absorbent and Mode 2 in Module 5

Exp. No.	Module No.	Mode of Oper.	Feed Pres. (kPa)	Feed Gas Comp.*	Purified Gas Comp.*	Purified Product Gas Flow Rate (cm ³ /min)
8-1	5	2	310 ~ 345	CO ₂ : 9.9%	CO ₂ : 1.005%	4
8-2	5	2	310 ~ 345	CO ₂ : 9.9%	CO ₂ : 1.05%	4 ~ 5
8-3	5	2	310 ~ 345	CO ₂ : 9.9%	CO ₂ : 1.12%	5
8-4	5	2	310 ~ 345	CO ₂ : 9.9%	CO ₂ : 1.28%	5 ~ 6
8-5	5	2	310 ~ 345	CO ₂ : 9.9%	CO ₂ : 1.41%	6 ~ 7
8-6	5	2	310 ~ 345	CO ₂ : 9.9%	CO ₂ : 1.69%	7 ~ 8
8-7	5	2	310 ~ 345	CO ₂ : 9.9%	CO ₂ : 1.86%	8
8-8	5	2	240 ~ 275	CO ₂ : 9.9%	CO ₂ : 0.95%	2 ~ 2.5
8-9	5	2	240 ~ 275	CO ₂ : 9.9%	CO ₂ : 1.06%	3.5 ~ 4
8-10	5	2	240 ~ 275	CO ₂ : 9.9%	CO ₂ : 1.27%	4.5
8-11	5	2	240 ~ 275	CO ₂ : 9.9%	CO ₂ : 1.40%	4.5 ~ 5
8-12	5	2	240 ~ 275	CO ₂ : 9.9%	CO ₂ : 1.50%	5

* Balance N₂

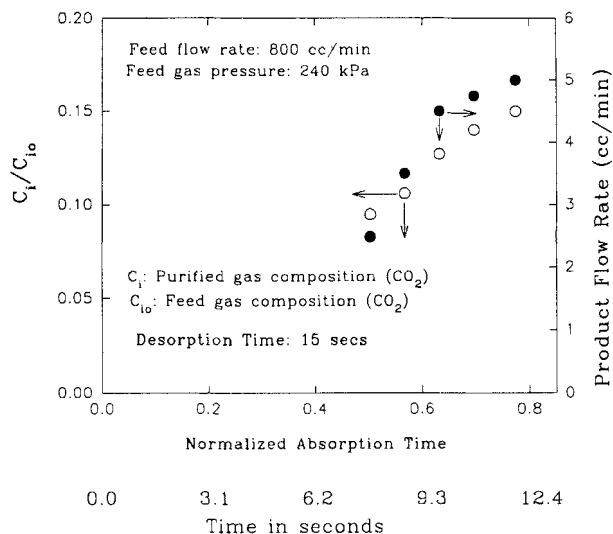


Figure 12. Removal of CO₂ with water as an absorbent in mode 2.

gas mixture was allowed to enter the module for 3 s; the purified gas mixture was taken out for different times. In the second set of experiments, feed gas mixture was allowed to enter the module for 2 s while the feed inlet metering valve was set at the same feed flow rate. A CO₂-N₂ mixture of 9.9% CO₂ and balance N₂ was used for all experiments. It was found that the extent of purification in the high-pressure purified gas mixture was higher when the feed gas was allowed into the module for only 2 s. The higher purification is most likely due to a longer gas mixture residence time when less amount of gas enters into the module. A desorption time of 15 s was used for all experiments. The experimental values of the normalized high-pressure exit composition and the purified gas flow rate for the second set of experiments (no: 8-8 to 8-12) have been plotted against the normalized absorption time ($D_{11}t/r_e^2$) in Figure 12.

Aqueous diethanolamine solution as an absorbent for CO₂ separation

A number of experiments were carried out using mode 3 and mode 2 for the absorption of CO₂ from a CO₂-N₂ mixture using a reactive 19.5 wt. % aqueous solution of DEA as an absorbent. Module 5 was used for all experiments using a feed gas mixture of 9.9% CO₂ and balance N₂. The time duration for absorption and desorption parts of the cycle in

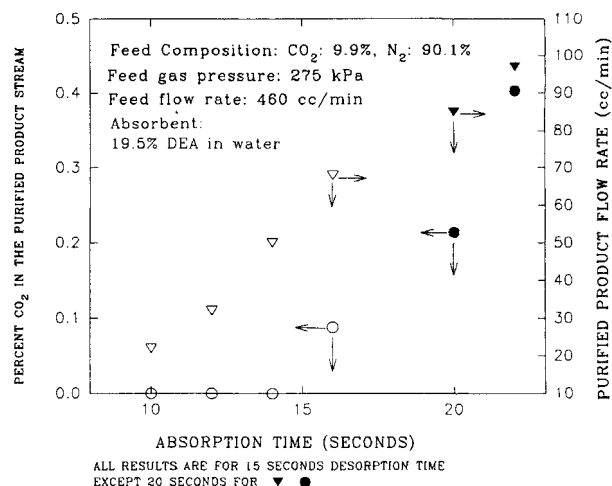


Figure 13. Removal of CO₂ with aqueous solution of DEA as an absorbent in mode 3.

mode 3, the feed flow rate, and the purified product flow rate for all runs are identified in Table 5 along with the purified gas composition. The feed gas flow rate was kept constant at 460 cc/min as the absorption time was changed. The CO₂ percentage in the purified product stream and the purified product flow rate are plotted against the absorption time in Figure 13. One observes that at this inlet feed flow rate, there was no CO₂ measured in the purified gas (as detectable by the GC) up to an absorption time of 14 s. When the absorption time is increased beyond 14 s, small amounts of CO₂ appear in the purified gas stream. It appears that 15 s of desorption time was enough for an absorption time of 16 s or lower. But for longer absorption periods, the desorption time was increased to 20 s to make the system stable. The results show a dramatic increase in the purification capability when a high capacity reactive absorbent like DEA is employed. Further, the rate of production of the purified gas was an order of magnitude higher when compared with water as absorbent.

Another set of experiments was carried out in mode 3 with a feed gas flow rate of 800 cc/min where a desorption time period of 20 s was used in all runs. Module 5 was used for all experiments using a feed gas mixture consisting of 9.9% CO₂ and balance N₂. The time duration for the absorption and desorption part of the cycle in mode 3, the feed flow rate, and the purified product flow rate for all runs are given in Table 6 along with the purified gas composition. The model

Table 5. Experimental Results for RAPSAB Using DEA Solution and Mode 3

Exp. No.	Module No.	Abs. Time (s)	Des. Time (s)	Feed Flow Rate (cm ³ /min)	Feed Pres. (kPa)	Product Outlet Comp.*	Product Flow Rate (cm ³ /min)
8.1-1	5	10	15	460	275	CO ₂ : 0.0%	20 ~ 25
8.1-2	5	12	15	460	275	CO ₂ : 0.0%	30 ~ 35
8.1-3	5	14	15	460	275	CO ₂ : 0.0%	50 ~ 55
8.1-4	5	16	15	460	275	CO ₂ : 0.088%	65 ~ 70
8.1-5	5	20	20	460	275	CO ₂ : 0.214%	~ 90
8.1-6	5	22	20	460	275	CO ₂ : 0.403%	~ 100

Feed Composition: CO₂: 9.9%, N₂: 90.1%
 * Balance N₂

Table 6. Experimental Results for RAPSAB Using DEA Solution and Mode 3 at a High Feed Gas Flow Rate

Exp. No.	Module No.	Abs. Time (s)	Des. Time (s)	Feed Flow Rate (cm ³ /min)	Feed Pres. (kPa)	Product Outlet Comp.*	Product Flow Rate (cm ³ /min)
10.1-1	5	10	20	800	~ 345	CO ₂ : < 50 PPMV	52.5
10.1-2	5	12	20	800	~ 345	CO ₂ : 500 PPMV	80
10.1-3	5	14	20	800	~ 345	CO ₂ : 1,000 PPMV	110
10.1-4	5	16	20	800	~ 345	CO ₂ : 0.2%	130
10.1-5	5	18	20	800	~ 345	CO ₂ : 0.4%	147.5
10.1-6	5	20	20	800	~ 345	CO ₂ : 0.8%	175
10.1-7	5	22	20	800	~ 345	CO ₂ : 1.2%	210
10.1-8	5	24	20	800	~ 345	CO ₂ : 2.5%	255

Feed Composition: CO₂:9.9%, N₂: 90.1%.
 * Balance N₂

simulation results have been compared with the experimental results for CO₂ separation using this 19.5% DEA solution in water as an absorbent. The comparison is shown in Figure 14 in terms of normalized high-pressure exit compositions plotted against the normalized absorption time ($D_{11}t/r_c^2$). The model results describe the experimental data well. (Table 7 provides the values of parameters used in the simulations.) The experimental values of the purified gas flow rate for different normalized absorption times are also given in the same plot. Note that CO₂ concentration is being reduced in these experiments from 10% level to less than 50 ppmv, that is, bulk separation to very high levels of purification. In fact, no CO₂ was detected in the GC in cases reported as < 50 ppmv.

We now consider experimental runs in the mode 2 type of operation; the duration of the open and close settings of the solenoid valves and the corresponding values of the feed gas pressure are given in Table 8. The purification results of each such run are provided in Figure 15. In these experiments, the feed flow rate was set at 1,500 cm³/min and the feed gas mixture was allowed to enter the module for 4 s; the purified gas was taken out for different times. If we compare these results with the results obtained from mode 3 type of operation, it could be concluded that mode 2 type of operation is

better than the mode 3 type of operation on the basis of the purified gas production rate. These results are further indicative of the considerable potential for RAPSAB as a gas purification technique.

The emphasis in this article was on the demonstration of a RAPSAB process and the objective was to remove CO₂ to purify feed N₂. However, if the objective is to concentrate the absorbed CO₂ as well, further modifications to the cycles are necessary (as is true for PSA systems). Such cycles have been developed using a hollow fiber module. The results of such cycles and an appropriate analysis will be reported later.

The proposed configuration may be useful for a variety of gas purification/separation systems. Some examples are: CO₂ removal from flue gas, purification of post-shift reactor synthesis gas to remove CO and CO₂ (this can be achieved using two consecutive RAPSAB processes), selective H₂S removal from a stream containing CO₂ and H₂S, and volatile organic compounds removal from solvent contaminated process air stream. Note that we have already demonstrated CO removal by such a RAPSAB process (Bhaumik et al., 1994).

Concluding Remarks

Rapid pressure swing absorption-separation of a gas mixture via nondispersive contacting of the feed gas with a non-wetting absorbent liquid in a microporous hydrophobic hollow fiber module has been demonstrated. The feed gas purification capability of such a process using reactive absorbents is extraordinary: 10% CO₂ level in N₂ is reduced to virtually zero CO₂ level (not detected by the GC whose lowest calibration was for 50 ppmv). The behavior of the adsorption part of this cyclic process can be modeled satisfactorily

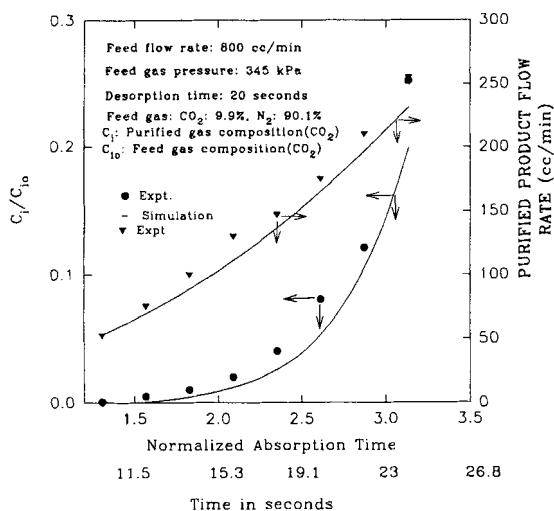


Figure 14. Removal of CO₂ with DEA as an absorbent in mode 3: experimental results vs. theoretical simulations.

Table 7. Parameters Used in the Simulation

Parameters	Values	Researchers
$D_{A, \text{water}}$	$1.92 \times 10^{-5} \text{ cm}^2/\text{s}$	Thomas and Adams, 1965
$D_{B, \text{water}}$	$3.00 \times 10^{-5} \text{ cm}^2/\text{s}$	Thomas and Adams, 1965
$H_{A, \text{water}}$	$3.71 \times 10^{-5} \text{ mol/cm}^3 \cdot \text{atm}$	Perry and Green, 1984
$H_{B, \text{water}}$	$6.31 \times 10^{-7} \text{ mol/cm}^3 \cdot \text{atm}$	Perry and Green, 1984
$D_{A, \text{DEA}}$	$1.44 \times 10^{-5} \text{ cm}^2/\text{s}$	Blanc and Demarais, 1984
$D_{B, \text{DEA}}$	$2.25 \times 10^{-5} \text{ cm}^2/\text{s}$	Blanc and Demarais, 1984
$H_{A, \text{DEA}}$	$3.97 \times 10^{-5} \text{ mol/cm}^3 \cdot \text{atm}$	Blanc and Demarais, 1984
$H_{B, \text{DEA}}$	$6.75 \times 10^{-7} \text{ mol/cm}^3 \cdot \text{atm}$	Blanc and Demarais, 1984
k_1	$1.41 \times 10^6 \text{ cm}^3/\text{mol} \cdot \text{s}$	Laddha and Danckwerts, 1981
$k_1 k_3 / k_2$	$1.20 \times 10^9 \text{ mol/cm}^3$	Laddha and Danckwerts, 1981

A: CO₂; B: N₂

Table 8. Settings of Solenoid Valves for Mode 2 Operation with Aqueous DEA Solution as an Absorbent

Exp. No.	Module No.	Mode of Oper.	Pres. in Fiber Lumen (kPa)	Valve No. 1 (s)		Valve No. 3 (s)		Valve No. 2 (s)		Total Cycle Time (s)
				Open	Close	Close	Open	Close	Open	
9.2-1	5	2	375	4	25	4	5	9	16	25
9.2-2	5	2	375	4	27.2	4	7.2	11.2	16	27.2
9.2-3	5	2	375	4	29	4	9	13	16	29

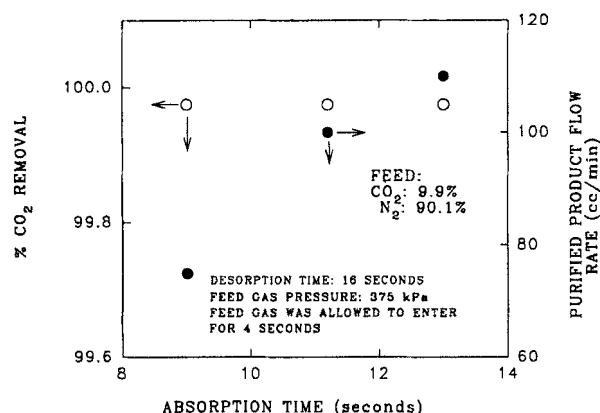


Figure 15. Experimental results for RAPSAB using DEA solution as an absorbent in mode 2.

from first principles for both water as well as the reactive liquid, an aqueous solution of DEA.

The potential of such a technique to integrate the best features of PSA, membrane contacting, and gas-liquid absorption may be fully realized if the desorption part of the RAPSAB cycle is developed further to improve the purity of the desorbed CO₂ stream. Further contamination of the gas phase by vapors of the absorbent liquid should be eliminated by appropriate choice of hollow fiber membranes.

Acknowledgment

The authors would like to thank Pittsburgh Energy Technology Center of the Dept. of Energy for support of this research under contract no. DE-FG22-90 PC 90300 in the University Coal Research Program. Helpful discussions with B.K. Dutta and A.K. Guha are acknowledged. Initial part of this project was carried out at Stevens Institute of Technology.

Notation

- $a = r_o/r_e$, dimensionless radial distance parameter
- C_i = concentration of species i in the purified gas stream, mol/m³
- C_{io} = concentration of species i in the inlet gas stream, mol/m³
- C_{jg} = concentration of species j in the gas phase, mol/m³
- C_{jl} = concentration of species j in the liquid phase, mol/m³
- d_i = inside diameter of a hollow fiber, m
- d_o = outside diameter of a hollow fiber, m
- D_{jg} = diffusion coefficient of species j in the gas phase, m²/s
- D_{jl} = diffusion coefficient of species j in the liquid phase, m²/s
- H_j = solubility coefficient of gas species j in a liquid, mol/(m³·Pa)
- k_1, k_2 = forward and backward rate constants for reaction 9
- k_3 = forward rate constant for reaction 10
- K_{jg} = gas-side mass-transfer coefficient of species j , m/s
- L = effective fiber length in a module, m
- N = total number of hollow fibers in a module
- r = radial distance, m

- r_e = equivalent radius of free surface, m
- r_i = inside radius of a hollow fiber, m
- r_o = outside radius of a hollow fiber, m
- r_s = inside radius of the module shell, m
- R = universal gas constant, (m³·Pa)/(mol·K)
- t = time, s
- T = temperature, K
- v_g = gas velocity in fiber lumen, m/s
- $X = z/L$, dimensionless longitudinal distance
- z = longitudinal distance, m

Greek letters

- ϵ = void fraction of the fiber bundle, m²/m²
- $\eta = r/r_e$, dimensionless radial distance
- θ = angular direction
- μ = viscosity, Pa·s
- $\pi = 3.14159...$
- $\tau = D_{j1}t/r_e^2$, dimensionless time parameter

Superscript and subscripts

- i = interface
- g = gas phase
- j = component j
- l = liquid phase
- u = upstream section

Literature Cited

- Beaver, E. R., and P. V. Bhat, "Integration of Membranes with Other Air Separation Technologies," *AIChE Symp. Ser.*, Vol. 84, No. 261, p. 113 (1988).
- Bhaumik, S., S. Majumdar, and K. K. Sirkar, "Rapid Pressure Swing Absorption Cleanup of Post-Shift Reactor Synthesis Gases," Final Report to DOE PETC, Pittsburgh, DOE Grant No. DE-FG22-90 PC 90300 (1994).
- Blanc, C., and G. Demarais, "The Reaction Rate of CO₂ with Diethanolamine," *Int. Chem. Eng.*, **24**(1), 43 (1984).
- Brian III, B. F., I. Zwiebel, and R. S. Artigue, "Numerical Simulation of Fixed-bed Adsorption Dynamics by the Method of Lines," *AIChE Symp. Ser.*, No. 259, p. 80 (1987).
- Gill, W. N., and B. Bansal, "Hollow Fiber Reverse Osmosis Systems Analysis and Design," *AIChE J.*, **19**(4), 823 (1973).
- Happel, J., "Viscous Flow Relative to Arrays of Cylinders," *AIChE J.*, **5**(2), 174 (1959).
- Karoor, S., "Gas Absorption Using Microporous Hollow Fiber Membranes," PhD Diss., Stevens Inst. of Technol., Hoboken, NJ (1992).
- Karoor, S., and K. K. Sirkar, "Gas Absorption Studies in Microporous Hollow Fiber Membrane Modules," *Ind. Eng. Chem. Res.*, **32**, 674 (1993).
- Keller, G. E., and R. L. Jones, "A New Process for Adsorption Separation of Gas Streams," *Amer. Chem. Soc. Symp. Ser.*, No. 135, p. 275 (1980).
- Kikkinides, E. S., R. T. Yang and S. H. Cho, "Concentration and Recovery of CO₂ from Flue Gas by Pressure Swing Adsorption," *Ind. Eng. Chem. Res.*, **32**, 2714 (1993).
- Kumar, R., and J. K. van Sloun, "Purification by Adsorptive Separation," *Chem. Eng. Prog.*, **85**(1), 34 (1989).
- Laddha, S. S., and P. V. Danckwerts, "Reaction of CO₂ with Ethanolamine: Kinetics from Gas Absorption," *Chem. Eng. Sci.*, **36**, 479 (1981).

- Papadopoulos, T. H., and K. K. Sirkar, "A Modified HFCLM Technique for Gas Separation at High Pressures," *J. Memb. Sci.*, **94**, 163 (1994).
- Perry, R. H. and D. W. Green, eds., *Perry's Chemical Engineers' Handbook*, 5th ed., rev., McGraw-Hill, New York, p. 3 (1984).
- Qi, Z., and E. L. Cussler, "Microporous Hollow Fibers for Gas Absorption. I. Mass Transfer in the Liquid," *J. Memb. Sci.*, **23**, 321 (1985).
- Sada, E., Z. Kumazawa, Q. Han, and H. Matsuyama, "Chemical Kinetics of the Reaction of Carbon Dioxide with Ethanolamines in Nonaqueous Solvents," *AIChE J.*, **31**, 1296 (1985).
- Sirkar, K. K., "Other New Membrane Processes," *Membrane Handbook*, Chap. 46, W. S. W. Ho and K. K. Sirkar, eds., Van Nostrand Reinhold, New York (1992).
- Spilman, R. W., "Economics of Gas Separation Membranes," *Chem. Eng. Prog.*, **85**(1), 41 (1989).
- Thomas, W. J., and M. J. Adams, "Measurements of Diffusion Coefficients of Carbon Dioxide and Nitrous Oxide in Water and Aqueous Solutions of Glycerol," *Trans. Faraday Soc.*, **61**, 668 (1965).
- Yang, R. T., *Gas Separation by Adsorption Processes*, Butterworths, Boston (1987).
- Yang, M. C., and E. L. Cussler, "Designing Hollow-Fiber Contactors," *AIChE J.*, **32**, 1910 (1986).

Manuscript received Sept. 26, 1994, and revision received Mar. 2, 1995.